Journal of Environment and Earth Science
ISSN 2224-3216 (Paper) ISSN 2225-0948 (Online)
Vol.10, No.2, 2020

Hydrological Impacts of Climate Change in Tikur Wuha Watershed, Ethiopian Rift Valley Basin

Mekin Mohammed[1*] Birhanu Biazn[2] Mulugeta Dadi Belete[3]
1.Ethiopian Institute of Agricultural Research (EIAR), Mehoni Agricultural Research Center, P.O. Box 71, Ethiopia
2.Senior Research Officer -Irrigation agronomist, International Crops Research Institute for Semi Arid Tropics (ICRISAT) C/O International Livestock Research Institute (ILRI), Box 5689, Addis Ababa, Ethiopia
3.Lecturer at Hawassa University, Institute of Technology, Hawassa, Ethiopia

Abstract
According to Intergovernmental Panel on Climate Change (IPCC) rising of global surface temperature, sea level rises, arctic and land ice decrease, erratic precipitation and increase of CO2 concentration are the main indicators of climate change. The main objectives of the study was to investigate the possible hydrological impacts of climate change on stream flow and sedimentation in Tikur Wuha watershed, by downscaling canESM2 (Canadian Earth System Model of second generation) global climate model using Statistical Downscaling Model (SDSM). Based on IPCC recommendation baseline periods (1987–2016) were used for baseline scenario analysis. Future scenario analysis was performed for the 2020s, 2050s, and 2080s. canESM2 model consists of Representative Concentration Pathway (RCP) RCP2.6, RCP4.5 and RCP8.5 scenarios. Impact assessment on stream flow and sediment yield was done by Soil and Water Assessment Tool (SWAT) hydrological model. SWAT model performance in simulating monthly stream flow for the study area was satisfactory with R^2 (0.77 and 0.87), N_{SE} (0.70 and 0.77) and D (-16 and -9) for calibration and validation periods respectively. The result of downscaled precipitation and temperature reveals a systematic increase in all future time periods for all three scenarios; RCP2.6, RCP4.5 and RCP8.5 scenarios. These increases in climate variables are expected to result in increase in mean annual stream flow of 8%, 13%, and 15 % for RCP2.6 scenario, 17%, 24%, and 31% for RCP4.5 scenario and 14%,24% and 35% for RCP8.5 scenario for the 2020s, 2050s, and 2080s, respectively. This leads to increment of sediment yield from different sub watershed. The estimated soil loss rate from different sub-watersheds had ranged from 0.42 tons/ha/yr to 28.31 tons/ha/year (1987-1999), whereas the annual weighted average soil loss rate from the watershed was estimated 16.80 tons/ha/year (2000-2100). Future work need to consider studying the effects of different climate change adaptation strategies.
Keywords: Climate change Scenarios, Ethiopia, Hydrological impact, SWAT model
DOI: 10.7176/JEES/10-2-04
Publication date: February 29th 2020

1. INTRODUCTION

1.1. Background

The Intergovernmental Panel on Climate Change (IPCC) defines climate change as in the state of the climate that can be identified by changes in the mean and/or the variability of its properties, and that continues for an extended period, decades or longer. It refers to any change in climate over time, whether due to natural variability or as a result of human activities (IPCC, 2007). The rising of global surface temperature, sea level rises, arctic and land ice decrease, erratic precipitation and increase of CO2 concentration are the main indicators of climate change. The shift in temperature and precipitation patterns affects the hydrology process and availability of water resource (IPCC, 2013).

Developing countries, particularly those in Africa are likely to be vulnerable to climate change as recurrent droughts, flood and siltation of water bodies continue to bring misery to millions in Africa (Nawaz *e*t al., 2010). The impact is worse for the contemporary African population where about 25% already experience water stress. Considering population increments and water use, it has been estimated that the portion of the African population at risk for water stress and scarcity will increase to 65% in 2025. Climate change is, however, expected to aggravate the current stress on water resources availability in Africa (Dile et al., 2013).

Studies at Bilate watershed in the Ethiopian Rift valley basin suggested that climate change could affect by decreasing of water resources (Tekle, 2014). Similarly, in Geba river basin shows the implication of reduced water availability and impacts on agricultural production (Ashenafi, 2014). On other hand, research conducted on Upper Blue Nile River Basin shows the positive change of precipitation in future (Mekonnen and Disse, 2016). Both researchers indicated that climate change strongly affects Ethiopian agriculture and socio-economic aspect.

Tikur Wuha watershed, located under the southern Rift valley basin of Ethiopia, contains the main tributary (Tikur Wuha river) of Lake Hawassa. To ensure the sustainability of Lake Hawassa, proper and sustainable management of this watershed is crucial. Thus, studying the hydrological impacts of climate change in Tikur Wuha watershed is very important though not studied yet. That is why this study was designed. The objectives of the

current study were: (1) to generate ensembles of future rainfall and temperature series using SDSM for a range of representative scenarios, (2) to simulate projected impacts of climate change on hydrological characteristics of the Tikur Wuha watershed using the hydrological model (SWAT).

2. MATERIALS AND METHODS

2.1. Description of study area

2.1.1. Location

The Tikur Wuha watershed approximately lies between $6^0$50'N-$7^0$10'N and $38^0$30'E-$38^0$44'30'E latitude and longitude respectively (Fig1) and covers a catchment area of 620.73 km^2. Its elevation ranges from 1688 to 2984masl. It contains Tikur Wuha River which is the upstream of Lake Hawassa drained from the Cheleleka Wetlands.

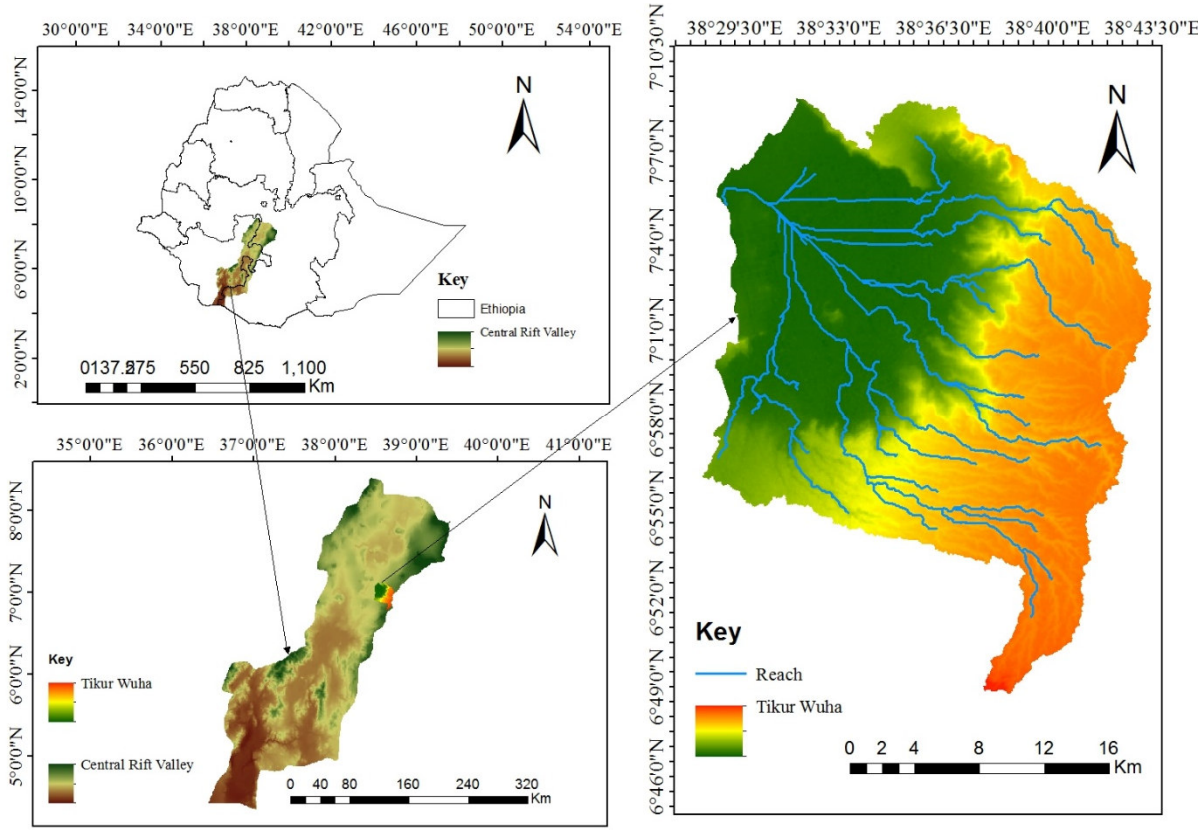

Figure 1: Location of Tikur Wuha watershed

2.1.2. Climate

Meteorological data collected from three different stations of the watershed indicated that the mean annual rainfall (mm) is 955.3, 1097.1 and 1150.4 in Hawassa, Haisawita and Wondo Genet College of Forestry and Natural Resources respectively (1987-2016). As indicated in Figure 2 below, the watershed has a bimodal rainfall pattern (Kebede *et al*., 2014). Maximum temperature showed 27.4ºC, 22.9ºC and 24.4ºC at Hawassa, Haisawita and Wondo Genet meteorological stations. Minimum temperature extends up to 13.1ºC, 11.3ºC and 9ºC at Hawassa, Haisawita and wondo Genet metrological stations respectively.

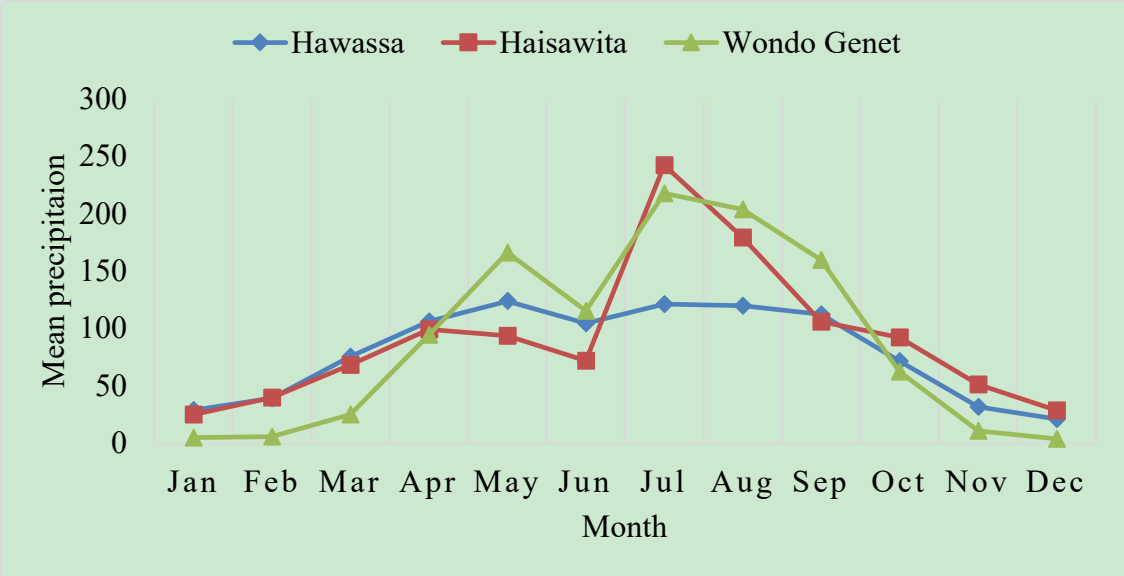

Figure 2: Mean monthly precipitation at Hawassa, Haisawita and wondo Genet Meteorological stations (1987-2016).

2.1.3. Topography

The watershed has marked topographic variation. The dominant slope classes are 8-15% and 15-30% covering about 54% of the total area. The slope class of 3-8% covers 21.6%, while the slope class of >30% covers 19% which is majorly the Northern, Easter and south Eastern escarpments of the sub watershed area. The remaining 5% of the total area is included in 0-3% slope class based on FAO slope classification for soil and water conservation (FAO, 2006).

2.2. Methodology

2.2.1. Data sources

Weather data were required for two purposes. First, the data were used for statistical downscaling model (SDSM), secondly the data were used as input to the SWAT (QSWAT) model for simulation of hydrological processes. Based on these objectives, daily maximum (Tmax) and minimum (Tmin) temperature and precipitation data were collected from Ethiopian National Meteorological Agency (NMA) for three metrological stations (Hawassa, Haisawita and Wondo Genet). Those three meteorological stations assumed as represent the whole watershed area. A single rain-guage station should represent an area that fulfills with the World Meteorological organization. As indicated by Dingman (2002) a single rainfall gauge density for tropical mountainous region is 300-1000 km^2/gauge. This study area gauge density is ranging from 59km^2/gauge to 221km^2/gauge is which enough to represent study area.

Stream flow and soil shapefiles were obtained from Ministry of Water, Irrigation and Electrification of Ethiopia. DEM and Landsat images downloaded from USGS Earth explorer.

2.2.2. Weather Data processing

Collected daily maximum temperature, minimum temperature and precipitation data has been weighted using Thiessen polygon technique of GIS (Enyew *et al*., 2014; Gumindoga *et al*., 2017; Liu *et al.,* 2017). Figure 3 shows the Thiessen polygons for Tikur_Wuha watershed showing the area of influence of each of the three weather stations: Hawassa (17.7%), Haisawita (38.51%%) and Wondo Genet (43.79%). Using this area coverage of each station weighted mean maximum temperature, minimum temperature and precipitation have been used for calibration, validation and scenario generation.

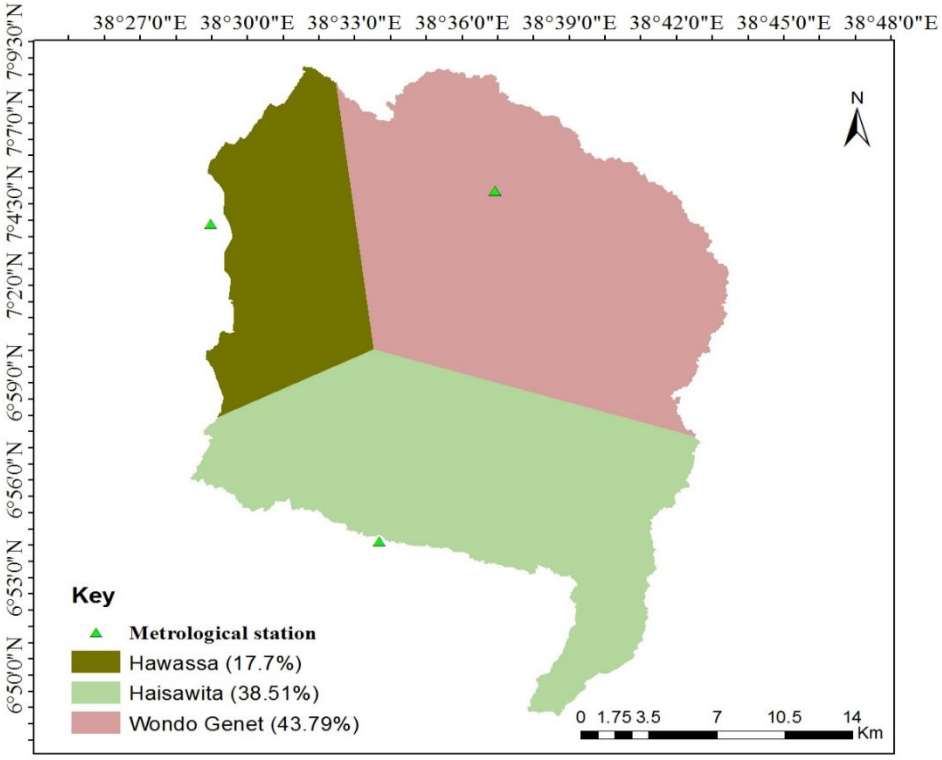

Figure 3: Thiessen polygons for Tikur wuha watershed

2.2.2.1. Weather generator data

Weather generator data of the study area was calculated using WGN excel macro. Download the WGN excel macro from SWAT (https://swat.tamu.edu/) to develop weather generator (WGEN user) for the study area.

2.2.3. Data quality checking

2.2.3.1. Filling of missing data

In this study, all metrological station daily data quality was checked to manage missed, suspended and outlier of the predictand data using SDSM.

After checking the data quality, Missing or gap record was filed using the well-known methodology of inverse distance weighing method (IDW) of GIS.

2.2.3.2. Consistency analysis

The consistencies of the data set of the given stations were checked using double mass-curve method with reference to their neighborhood stations.

2.2.3.3. Screening the downscale predictor variables

The choice of appropriate downscaling predictor variables was under taken through the screen variable option of SDSM using correlation analysis, Partial correlation analysis, and scatter plot partial correlation analysis was done for selected predictors to see the level of correlation with each other. This statistics identify the amount of explanatory power of the predictor to explain the predictand (Wilby and Dawson, 2007). Finally, the scatter plot was carried out in order to identify the nature of the association (linear, nonlinear, etc.), whether or not data transformation(s) may be needed, and the importance of outliers.

2.2.4. Spatial data processing

The spatial data set were projected in addendum UTM Zone 37, which is the transverse Mercator projection parameter for Ethiopia, using QGIS 2.6. The land uses/covers data were reclassified for QSWAT2012 database from landsat8 for the study area map. In addition to map preparation, the land use lookup table was prepared with SWAT code of land use database.

The soil database were extracted and collected from Harmonized World Soil Database (HWSD) and FAO soil Classification of world soil. The collected soil properties were edited to QSWAT2012 soil database. After the soil database has been adjusted for QSWAT software, the soil lookup table has been prepared with similar names of the database.

The digital elevation model (DEM) is one of the input data for QSWAT model. For this study, the digital elevation model was downloaded from Earth Explorer-USGS (https://earthexplorer.usgs.gov/). The grid resolution lies at 30*30 m. It is necessary for the stream network processing in SWAT model.

2.5. Climate and Hydrological modeling approach

Two modeling approaches were used in this study. The first part was climate change modeling approach and the second was hydrological modeling approach. The model outputs were finally analyzed, summarized and presented as maps, graphs and tables.

2.6. General circulation model (GCM) set up and climate change scenarios

Climate change scenario was obtained from GCM the World Climate Research Program's (WCRP's) Coupled Model Inter-comparison Project phase 5 (CMIP5) multi-model dataset (Wilby and Dawson, 2007). For this study, canESM2 (Canadian Second Generation Earth System Model) which was freely available at the Canadian climate change scenario group website **(***http://ccdsdscc.ec.gc.ca/?page=pred-canesm2***)** was used and downscaled to the site level using the Statistical Downscaling Model (SDSM).

The model results were available for RCP2.6 (low emission), RCP4.5 (medium to low emission) and RCP8.5 (high to medium emissions) scenarios (Wayne, 2013). The result was used to produce the future scenario. This model was applied in this study because of the following reasons. Firstly, the GCM model is widely applied in many climate change impact studies. The results of CanESM2 can be easily downscaled using SDSM (Dile *et al.,* 2013) and the model provides daily predictor variables which can be used for the Statistical Downscaling Model. Secondly, it provides large scale daily predictor variables which could be used for the statistical downscaling model (SDSM) (Wilby and Dawson, 2007). Thirdly, a single run was downloaded for each scenario, and data were extracted for the pixel containing the observation stations. Lastly, the model has given 20 ensemble model result when statistically downscaled and correctly used RCP scenario that have high climate mitigation policy (Riahi *et al*., 2007) and RCPs offer a better understanding in terms of the concentration of future greenhouse gases for running climate models than previous scenarios (Meinshausen *et al*., 2011).

2.6.1. Downscaling techniques

For this study, SDSM 4.2.9 decision support tool for the assessment of regional climate change impacts developed by Wilby and Dawson (2007) was used to downscale large-scale predictors and it was freely downloaded from http://www.sdsm.org.uk.

SDSM develops statistical relationships, based on multiple linear regression techniques, between large-scale (predictors) and local (predictand) that is precipitation and maximum and minimum temperature for this study which could be used as input for hydrological modeling.

2.6.2. Predictor variables

Large-scale predictor variable information is freely obtained from the Canadian climate impact scenario group with web address of: *http://ccdsdscc.ec.gc.ca/?page=pred-canesm2*. The National Center for Environmental Prediction (NCEP_1961-2005) reanalysis data and CanESM2 predictor variables for the RCP2.6, RCP4.5 and RCP8.5 are obtained on a grid by grid box basis from a resolution of 2.5° latitude by 3.75° longitude. Since the geographical location of the watershed is between $6^0$50'N-$7^0$10'N and $38^0$30'E-$38^0$44'30''E latitude and longitude respectively, the required predictor data that represents the watershed were downloaded from the nearest average location of the watershed (Wilby and Dowson, 2007).

2.6.3. Screening the downscale predictor variables

The choice of appropriate downscaling predictor variables was undertaken through the screen variable option of SDSM using correlation analysis, Partial correlation analysis, and scatter plot partial correlation analysis for selected predictors to get the level of correlation with each other. These statistics identify the amount of explanatory power of the predictor to explain the predictand (Wilby and Dawson, 2007). Finally, the scatter plot was carried out to identify the nature of the association (linear, nonlinear, etc.), whether or not data transformation(s) may be needed, and the importance of outliers.

SDSM model has two processes called conditional and unconditional processes to be specified before the analysis takes place. In case of daily temperature where the predictand-predictor process is not regulated by the intermediate process, so, the unconditional process was used, whereas, for daily precipitation where the amounts depend on the occurrence of wet-day, the conditional process was chosen (Benestad *et al*., 2008). Significance value is used to test the significance of predictor–predictand correlations and it was set as the default of the probability level at 0.05 ($p<0.05$).

Several analyses were made by selecting a maximum of 6 out of 26 predictor variables at a time till best predictor-predictand correlations were found even though up to 12 predictors are possible to select at a time (Wilby and Dowson, 2007).

2.6.4. Model calibration and validation

The model was calibrated for precipitation and maximum and minimum temperature (predictand variables) along with a set of predictor variables and computed the parameters of multiple regression equations with an optimization algorithm. Daily data were used for model calibration for data representing the current climate condition of the period 19 years (1987–2005). The event threshold was set to 0°C for temperature and 0.1 mm/day for precipitation in order to treat trace rain days as dry days (Wilby and Dawson, 2004).

Validation was done based on 11 years of simulation for years 2006–2016. Validation of the model was performed using the results of the weather generator and independent observed data that were used for calibration.

2.6.5. Scenario generation

The period from 1987-2016 were considered as a base period whereas the period from 2017-2100 were considered as future periods. The future periods have been divided into three time horizons; from the 2020s (2017-2044), 2050s (2045-2072), and 2080 (2073-2100) and analyses were made for each time horizons.

2.7. Hydrological (SWAT) model setup and analyses

SWAT is a semi-distributed, continuous time, rainfall runoff model developed by the USDA Agricultural Research Service (ARS) and simulations are performed using a daily time step. In addition, the movement of water, sediment, and agricultural chemical yields are simulated depending on varying soils, land use and management in complex watersheds over long time periods (Dixon and Earls, 2012).

After the data was collected and prepared, the model setup was done for all input data by following five steps which were used for SWAT model setup: (1) watershed delineation, (2) HRU definition, (3) weather data definition, (4) parameter sensitivity analysis, and (5) calibrations and model performance evaluation.

3. RESULT AND DISCUSSION

3.1. Predictor variable selection

Predictor variables that have better spatial and temporal correlation with the predictand of all weather parameters for the study area at significance level of less than 0.05 are presented in Table 1. The application of these empirical predictor-predictand relationships of the observed climate is to downscale ensembles of the same local variables for the future climate. This is based on the assumption that the predictor-predictand relationships under the current condition remain valid under future climate conditions.

Table 1: List of predictor variables that had better spatial and temporal correlation with the predictands at significant level of less than 0.05($p<0.05$).

Predictand	Predictorors (NCEP reanalysis)	Symbol	Parti.corr(R)	P valu
Maximum Temperature	Surface air flow strength	ncepp1_fgl.dat	-0.093	0
	Surface zonal velocity	Ncepp1_ugl.dat	-0.067	0
	Surface divergence	Ncepp1zhgl.dat	-0.022	0.03
	850 hpa zonal velocity	Ncepp8_ugl.dat	-0.033	0.00
	850 hpa geo potential height	Ncepp850gl.dat	-0.185	0
	Specific humidity at 500hpa	Nceps500gl.dat	-0.133	0
	Specific humidity at 850 hpa	Nceps850gl.dat	-0.233	0
Minimum temperature	Mean sea level pressure	ncepmslpgl.dat	-0.108	0
	Surface air flow strength	ncepp1_fgl.dat	-0.078	0
	Surface velocity	ncepp1_Zgl.dat	-0.019	0.0821
	500hpa wind direction	ncepp5thgl.dat	-0.071	0
	850 hpa air flow strength	ncepp8_fgl.dat	-0.031	0.0031
	Specific humidity at 500hpa	nceps500gl.dat	-0.019	0.0851
	Surface specific humidity	ncepshumgl.dat	0.032	0.0021
Precipitation	Mean sea level pressure	ncepmslpgl.dat	-0.028	0.1109
	Surface Meridians velocity	ncepp1_vgl.dat	-0.047	0.0069
	Surface velocity	ncepp1_zgl.dat	-0.002	0.5583
	500 hpa zonal velocity	ncepp5_ugl.dat	-0.081	0
	500 hpa meridians velocity	ncepp5_vgl.dat	-0.146	0
	850 hpa meridians velocity	ncepp8_vgl.dat	-0.076	0
	850 hpa geo potential height	ncepp850gl.dat	0.047	0.0067
	Specific humidity at 500hpa	nceps500gl.dat	-0.001	0.5627

Hence, hpa is a unit of pressure, 1 hPa = 1 mbar = 100 Pa = 0.1 kPa.

The result of predictor-predictand selection indicate that the partial correlations of surface air flow strength has the strongest association with maximum and minimum temperature. In addition, maximum and minimum temperatures are strongly correlated with 850 hpa geo potential height, which shows their heavy dependence on regional temperatures. Since the partial correlation coefficient (r) shows the explanatory power that is specific to each predictor, all are significant at $p \leq 0.05$.

3.1.4. Model calibration and validation

The SDSM calibration was done for the period of 19 years (1987-2005) at a monthly model type in order to see the monthly temporal variations. The results showed that, the simulated precipitation, maximum and minimum temperature had good agreements with the observed results. The overall agreement was good which are located in Table 2.

Table 2: Calibrated and validated precipitation, maximum and minimum temperature

Predictands	R^2	
	Calibration	Validation
Precipitation	0.94	0.95
Maximum temperature	0.97	0.99
Minimum temperature	0.92	0.98

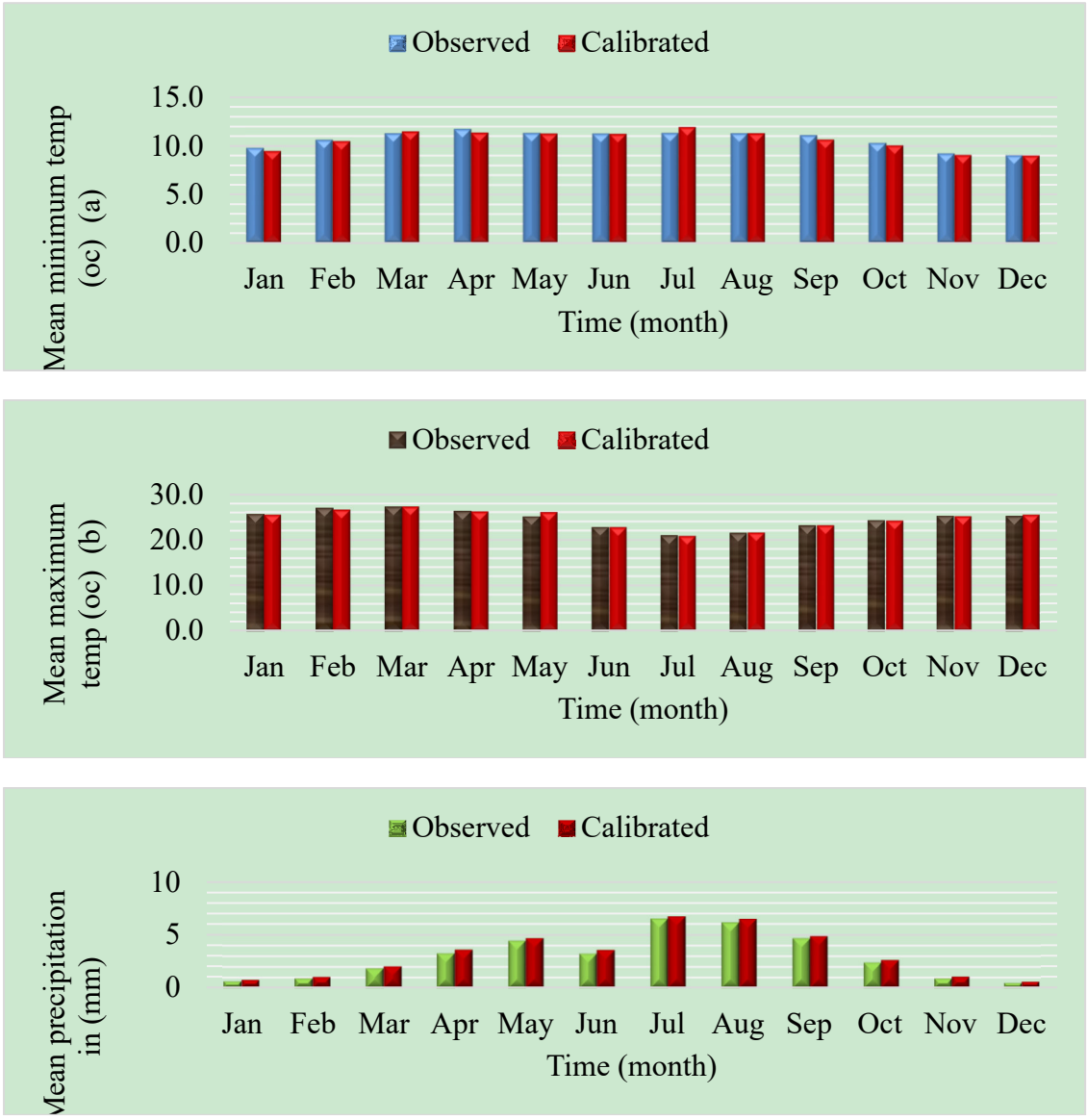

Figure 4: Calibrated and observed mean daily minimum temperature (°C) (a) and mean daily maximum temperature (°C) (b), mean daily precipitation (mm) (c) in the time step in Tikur wuha watershed.

Validation was done using an independent observed data for the period of eleven year from 2006 to 2016. Here also twenty ensembles (runs) of daily values were generated and the averages of these ensembles were taken for the comparison. The correlation coefficients that were found during the calibration are also maintained during the validation as shown in Table 2. A good agreement was also found between the observed and simulated precipitation (R^2=0.94 and 0.95 for calibration and validation) though it is a conditional process and for minimum and maximum temperature were R^2 =0.92 and 0.97 respectively during calibration.

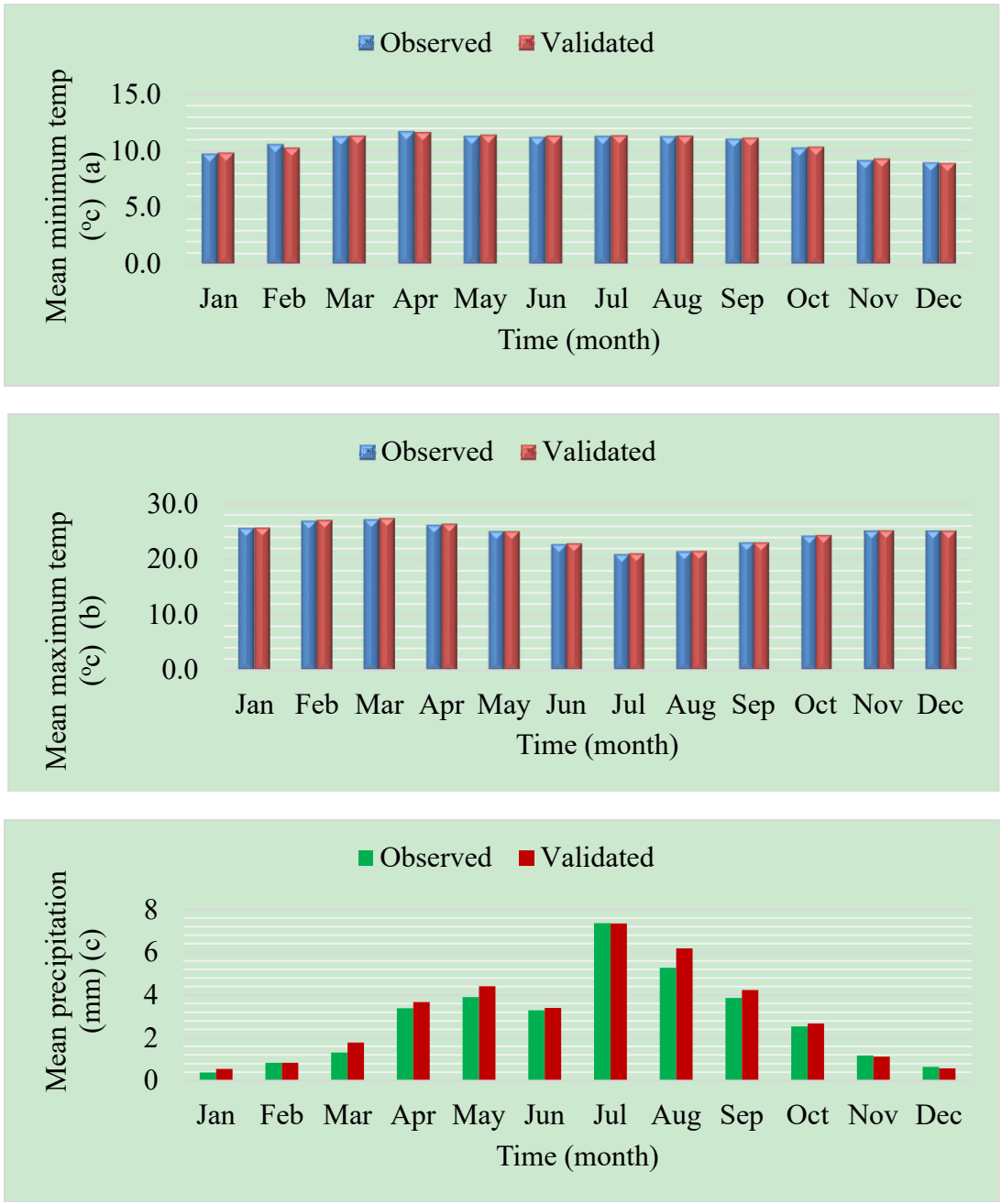

Figure 5: Validated and observed mean daily minimum temperature (a), maximum temperature (b) and precipitation (c)

3.2. Future climate change Scenario generation

The climate scenario for the future period was developed from statistical downscaling using the GCM predictor variables for the three emission scenarios for 84 years based on the mean of 20 ensembles. The analysis was done based on 28 years period from 2017-2044, 2045-2072 and 2073-2100. The IPCC recommends 1986-2005 as a climatological base period in impact assessment. In this study baseline period climatic condition is analyzed based on meteorological station records of the study area. Hence, for this research, the period from 1987-2016 was taken as a base period within which the comparison was made. The observed climatological data collected from Ethiopian meteorological agency contain more consistent time series records from the period 1987 and onwards than the period before 1987 and this is why the period from 1987-2016 was taken as a base period.

3.2.1.Minimum temperature

As it can be seen from Figure 6 (a, b and c), the results for annual mean minimum temperature showed an increasing trend for both scenarios (RCP2.6, RCP4.5 and RCP8.5) from 2017 to 2100. With respect to monthly minimum temperature, the downscaled minimum temperature scenario indicates that there might be an increasing

trend on the months of January, June and July for RCP2.6 scenarios from 2017 to 2100. But March (2045-2100), August (2017-2072), September and November (2017-2100) months shows a decreasing trend for RCP2.6 scenario. In the RCP4.5 scenario the projected minimum temperature shows an increasing trend in January, February, June and July months from 2017-2100. But from August to December the minimum temperature shows a decreasing trend from 2017-2100 except October (a slight increase on 2017-2044). In the RCP8.5 scenario the minimum temperature shows an increasing trend on January, February, June, July, and October months from 2017-2100. But April, May, August, November and December months showed a decreasing trend from 2017-2100. The highest increment of minimum temperature was projected on RCP8.5 scenario in the month of January +3.09°C, +3.09°C, and +3.26°C for the 2020s, 2050s and 2080s periods respectively. The annual minimum temperature showed an increasing trend which is in line with previous study conducted on Bilate watershed of the Central Rift Valley of Ethiopia (Tekle, 2014).

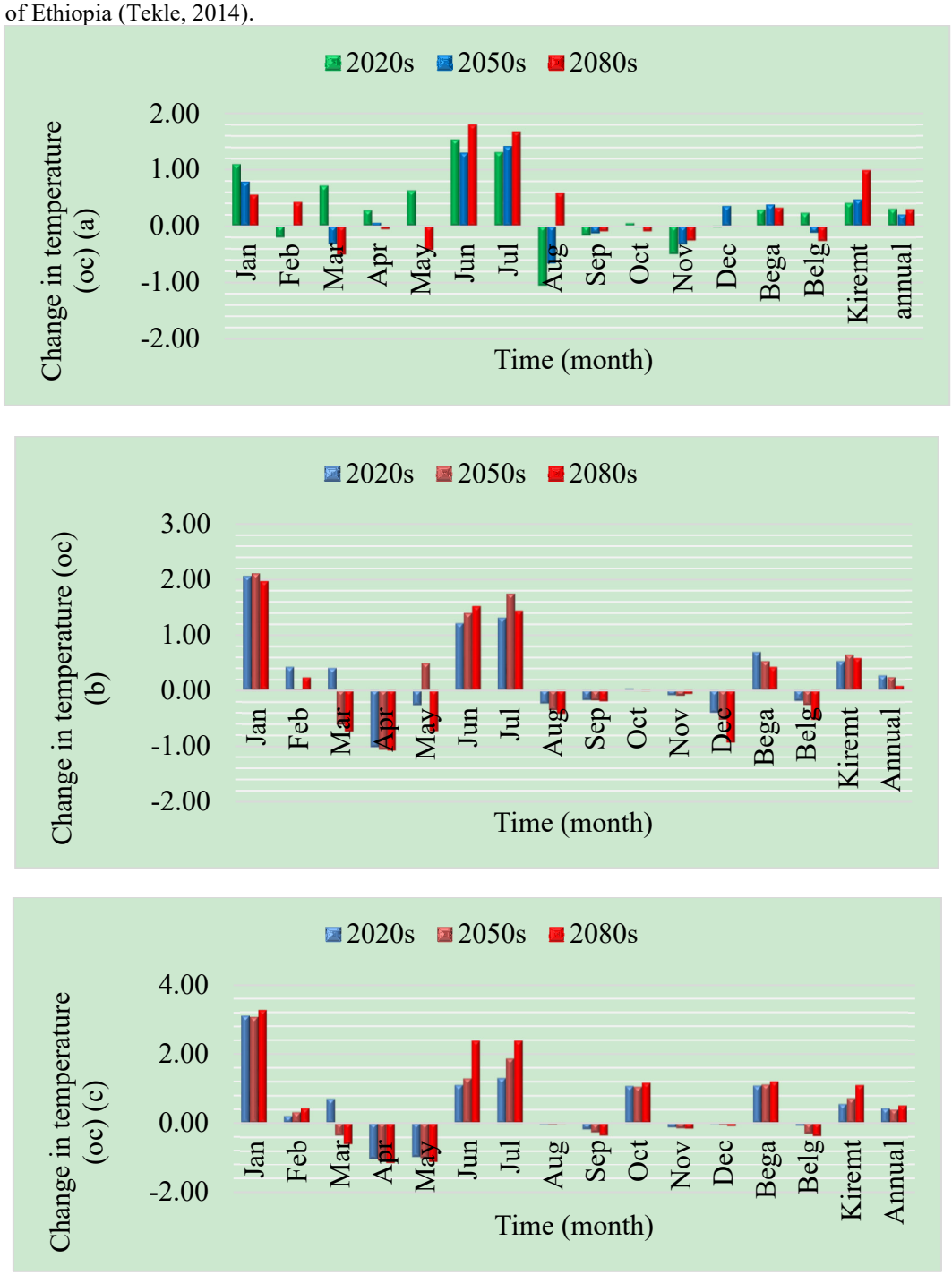

Figure 6: Change of downscaled monthly minimum temperature from the baseline period for canESM2 RCP2.6 (a), RCP4.5 (b) and RCP8.5 (c)

3.2.2. Maximum temperature

The mean monthly, seasonal and annual change in maximum temperature for the future period (2017-2100) for both RCP2.6, RCP4.5 and RCP8.5 scenarios are shown in Figure 7 (a, b, c). As it can be seen from Figure 7, the results (2017-2100) for annual mean maximum temperature showed an increasing trend for the three scenarios (RCP2.6, RCP4.5 and RCP8.5) from 2017 to 2100. With respect to monthly maximum temperature, the downscaled maximum temperature scenario indicates that there might be an increasing trend from January to April and from October to December for both scenarios (RCP2.6, RCP4.5 and RCP8.5) from 2017 to 2100. But from May to September the projected maximum temperature shows a decreasing trend for both scenarios except July (a slight increase for RCP8.5 for 2020s). The highest increment of maximum temperature was projected in the month of October, +1.9°C for RCP8.5 scenario. The increment was higher but not worth based on IPCC-TGICA, (2007) in which the globally averaged surface air temperature was projected to warm 1.4°C to 5.8°C by 2100.

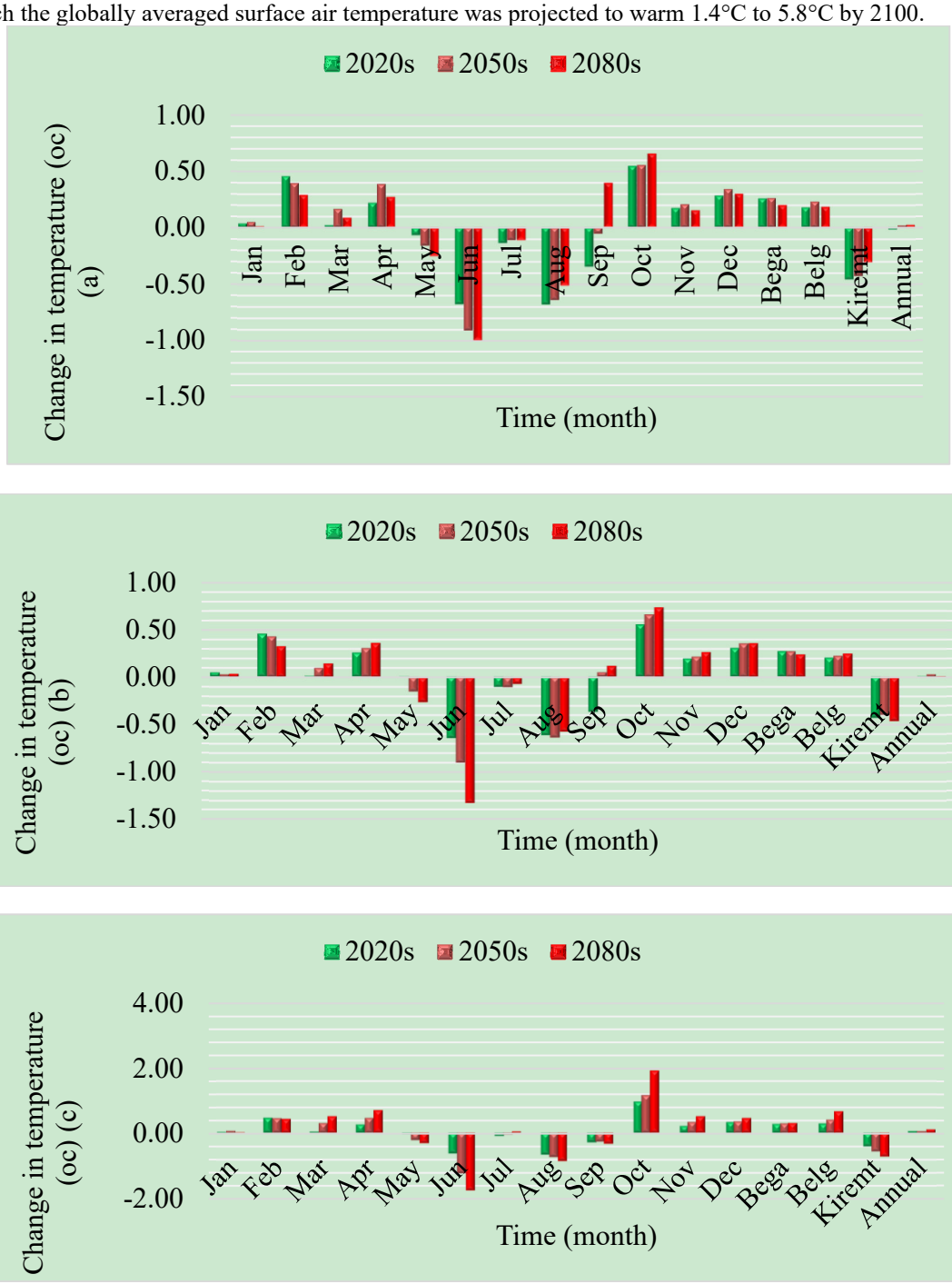

Figure 7: Change of downscaled monthly maximum temperature from the baseline period for canESM2 RCP2.6 (a), RCP4.5 (b) and RCP8.5 (c)

3.2.3.Precipitation

As it can be seen from Figure 8 (a, b and c) the results (2017-2100) for annual percentage change in precipitation showed an increasing trend for the three scenarios (RCP2.6, RCP4.5 and RCP8.5). In 2020s (2017-2044) the increment of annual percentage change of precipitation were from +13.8%, +14% and +13.2% for RCP2.6, RCP4.5, and RCP8.5 scenario respectively. In 2050s (2045-2072) the increment of annual percentage change of precipitation were +14.6%, +15.4% and +17.4% for RCP2.6, RCP4.5 and RCP8.5 scenario respectively. In 2080s (2073-2100) the increment of annual percentage change of precipitation were +16%, +15.4% and +19.44% for RCP2.6, RCP4.5 and RCP8.5 scenario respectively.This increement indicate similar result with IPCC-TGICA, (2007) that rainfall increase or decrease (up to ±20%) in 2100.

The results of this study was thus in line with the previous researches done on upper Blue Nile basin, Tana basin, Bilate catchment of Central Rift Valley Basin of Ethiopia (Kim *et al*., 2008, Taye, 2010, Tekele, 2014). Moreover, UNFCC (2007) assessed regional impacts and vulnerabilities to climate change in four regions including Africa and the results showed that annual mean rainfall would increase in East Africa due to climate change.

On monthly basis, the percentage change in precipitation is not systematic, i.e precipitation increases in some months and decreases in some other months. The percentage changes in precipitation increases from July to November, January and March monthes. But decreases in February, April and June months for the future (2017-2100) periods for all senarios. The increment is most dramatic in January for both RCP2.6, RCp4.5 and RCP8.5 scenarios in which the precipitation increases by 67% (2050s), 40% (2050s) and 70.5% respectively. The decrease in precipitation on the month of February which reaches to a maximum of 43% (2073-2100), 45% (2073-2100) and 43.4% (2073-2100) for RCP2.6, RCP4.5 and RCP8.5 scenario respectively.

Seasonally, the precipitation increases in Belg (February-May), and Kiremit (June-September) in which the precipitation increases up to a maximum of 12% (2073-2100) for RCP2.6 scenario, 16% (2073-2100) for RCP4.5 scenario and 20% (2073-2100) for RCP8.5 scenario in the Belg season and 21% (2017-2044) for RCP2.6 scenario, and 20% (2017-2044) for RCP4.5 scenario and 20.23% (2045-2072) for RCP8.5 scenario in the Kiremit season. A study done by Rizwan *et al*. (2010) on Blue Nile based using HadCM3 model also showed that, the mean precipitation increases in Kiremt season for both A2 and B2 scenarios which is in line with this study (RCP2.6, RCP4.5 and RCP8.5 scenarios). Moreover, in Kiremit season the average precipitation projections for the entire Nile basin (2020 and 2080) by Beyene *et al*. (2010) showed increasing trends. Belg and Kiremt seasons, the average precipitation projections on Gilgel Abay River (2020, 2050 and 2080) by Dile *et al*. (2013) showed increasing trends. The increment of precipitation in Belg and Kiremit season may have an opportunity for agriculture since these two seasons are the cropping season in Ethiopia as well as Rift vally basin. Precipitation decreases in Bega (October–January) season by 6.28% (2017-2044) and 6.31% (2073-2100) for RCP2.6, 9.5% (2017-2044) and 1.8% (2073-2100) for RCP4.5 scenarios. In addition, for RCP8.5 scenarios the the precipitaion showed increasing trends for 2050s and 2080s scenarios, but a slight decreament on 2020s scenario.

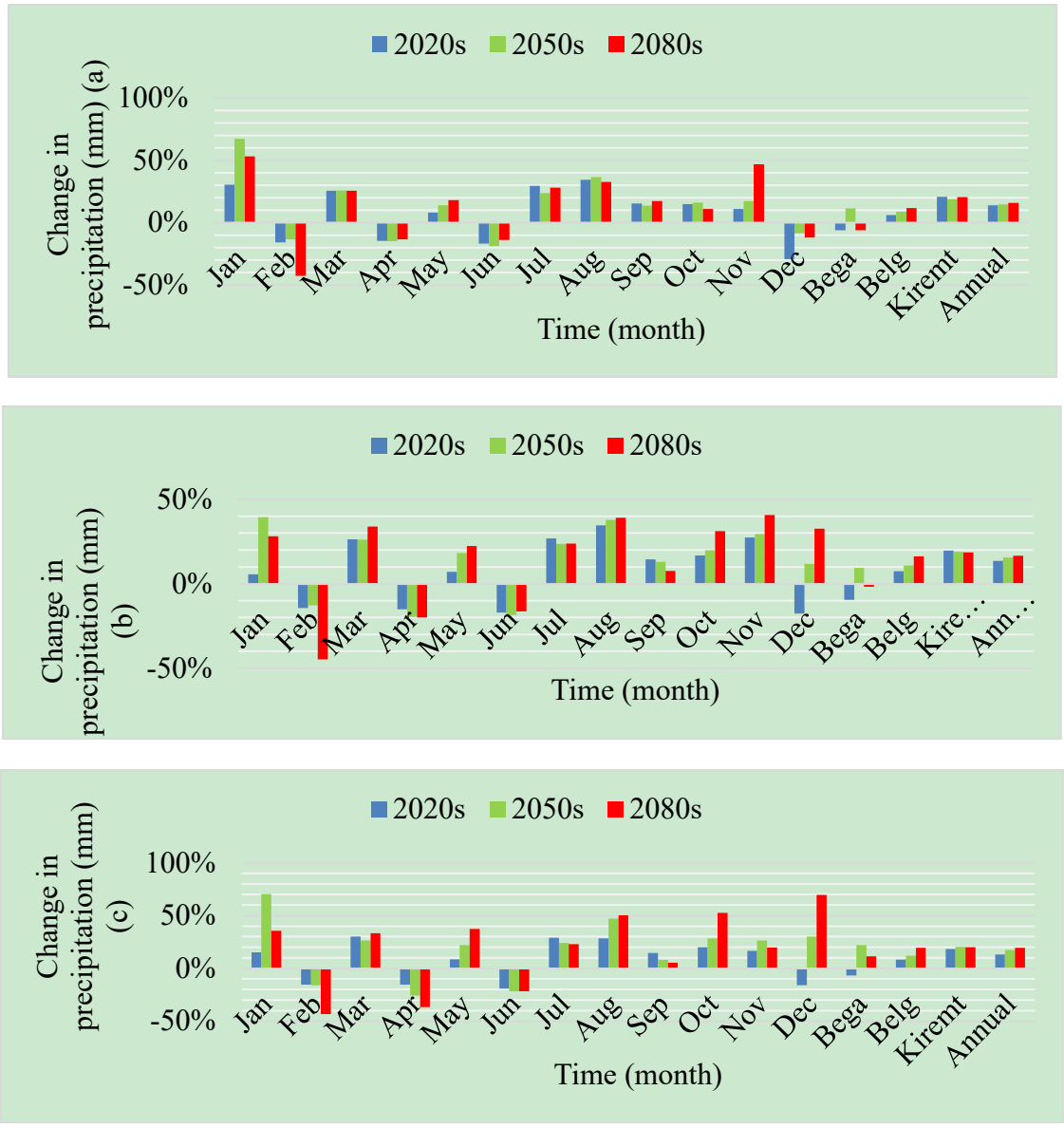

Figure 8: Percentage change in monthly, seasonal and annual precipitations in the future (2017-2100) for RCP2.6 (a), RCP4.5 (b) and RCP8.5 (c) scenario from the base period

3.3. SWAT Hydrological Model

3.3.1. Watershed characteristics

3.3.1.1. Watershed delineation and HRU definition of model input

The Tikur Wuha watershed has an area of 62073 ha which resulted in 69 sub watersheds having 548 HRUs. The sub-basins area calculated from the total watershed ranged in 7.0 ha (sub basin 56) to 2861.8ha (Sub basin 51), with an average of 1434.4ha. Among 69 sub-watersheds, 19 have area under 500ha, 26 sub-watersheds have area between 500 and 1000ha, 17 sub watersheds have area between 1000-2000ha and the rest 7 sub-watersheds have area between 2000 and 2861.8ha.

SWAT divide all sub basins up in to one or more representative HRUs by defining and overlaying the land use, soil type and slope of the study area sub watersheds. In order to balance the representation detail of land use, soil and slope with the complexity caused by increase number of HRUs, thresh hold values were determined for land use (15%), soil (10%), and slope (15%) in this study.

The total 548 HRUs resulted in the model had a minimum size of 0.78 ha and maximum of 129.81 ha with an average HRU of 10.38 ha. The redefined result of DEM of the area by SWAT model used in HRUs distribution of sub-basin is located in Figure 9.

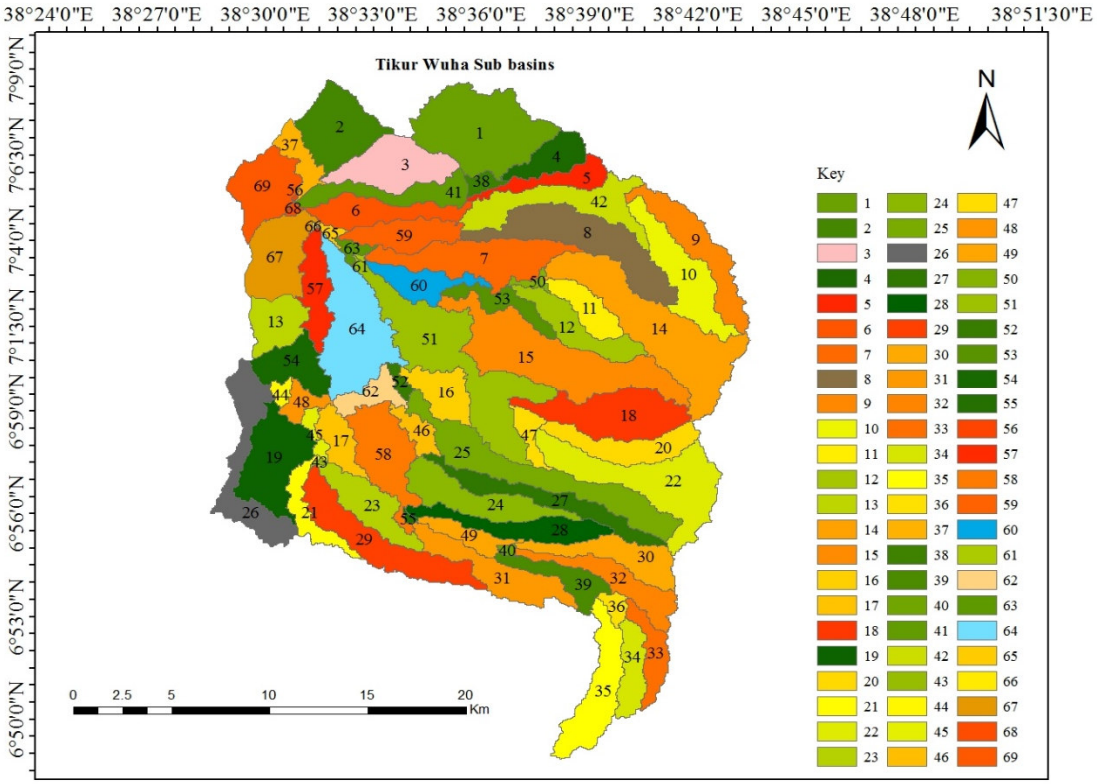

Figure 9: Sub basin of Tikur Wuha watershed

3.3.1.2. Land use/land cover characterization

Six land use/land cover types were identified using Landsat images which is downloaded from Earth Explorer-USGS (https://earthexplorer.usgs.gov/), December 12,2017 Landsat8 images. After image processing, land use/cover map was developed which has an overall classification accuracy of 85.71% and kappa statistic of 0.79 using ERDAS IMAGINE 2015. As it can be observed in Figure 10, most portion of the watershed was covered with cultivated and Forest land, which accounts for 46.6% and 23.6% respectively of watershed area.

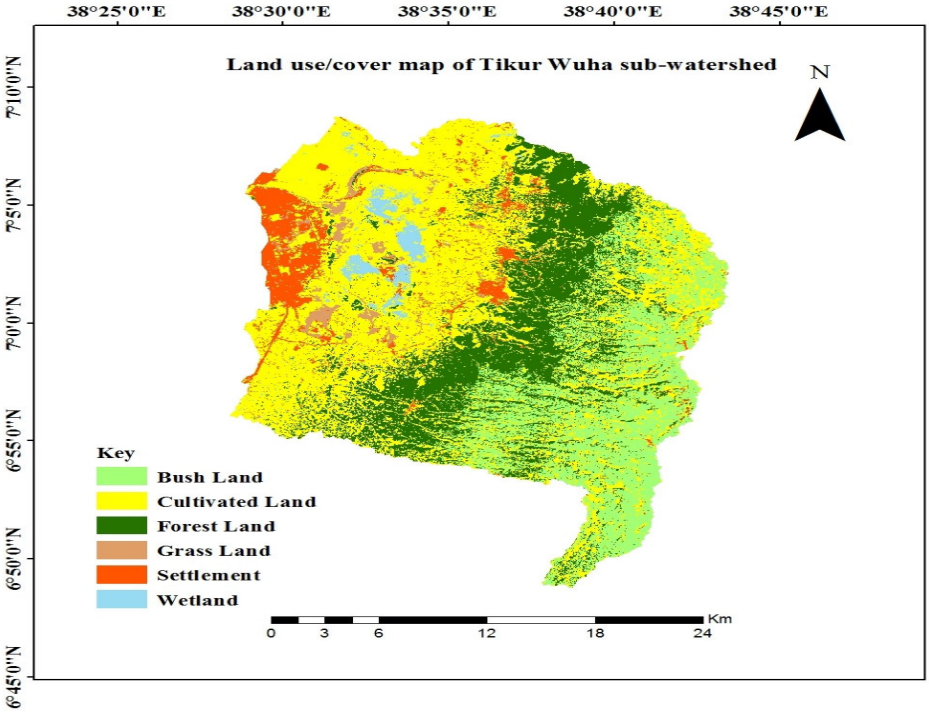

Figure 10: Land use/cover type of Tikur Wuha watershed

3.3.1.3. Soil characterization

The soil group classified in the study area is shown in Figure 11 as Leptosol, Vertic cambisol, Vertic Luvisol, Vitric Andosol, Haplic Luvisol and Eutric Cambisol . Major type of soils are Vertic Luvisol and Haplic Luvisol covering an area of 24584.8 ha and 24307.2 ha and accounting for 39.6% and 39.2% respectively of Tikur Wuha watershed.

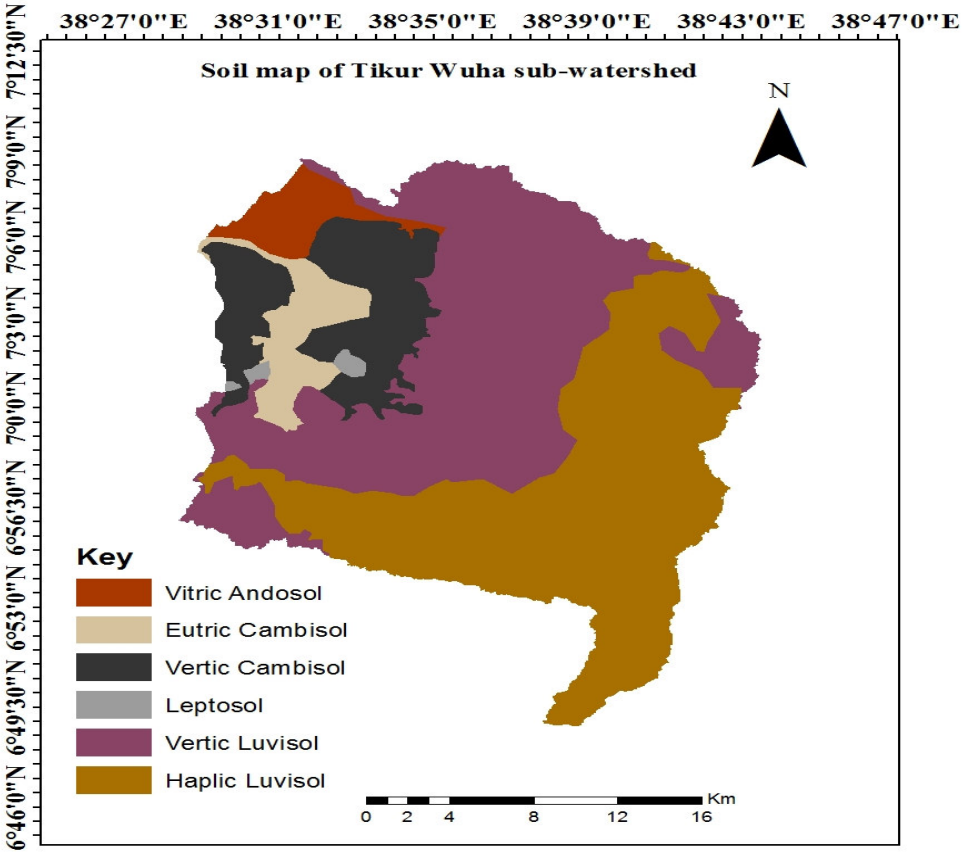

Figure 11: soil type of Tikur Wuha watershed
Source: Shapefile from Ministry of water, irrigation and electrification of Ethiopia

3.3.2. Model sensitivity analysis

Sensitivity analysis was carried out before calibrating the model to save time during calibration. In this study, identifying sensitive parameters enables to focus only on those parameters which affect most the model output during calibration since SWAT model has a number of parameters to deal with. Some parameters do not have any influence on the model output while some may have little effect.

3.3.3. Parameters sensitive to stream flow

Impact assessments on stream flow were done by soil and water assessment tool (SWAT) hydrological model with different sensitivity parameters. Even though there were more than 26 sensitivity parameters those were used for stream flow calibration, around 12 parameters were selected for this study. Those 12 parameters are sensitive, were used to calculate the amount of flow from the watershed. The parameter identification was done by using the monthly flow data from 1987 to 1994.

SWAT-CUP global sensitivity analysis has been carried out for the parameters. According to the result from the global sensitivity analysis, initial Soil Conservation Service (SCS) runoff curve number for moisture condition II (CN2) was found to be the most sensitive parameter followed by Ground water delay (GW_DELAY), Soil evaporation compensation factor (ESCO), Saturated hydraulic conductivity (SOL_K) and Soil bulk density (SOL_BD) ranking up to fifth position. Based on the analysis result, Available water capacity (mm water/mm soil) (SOL_AWC), Base flow recession constant (ALPHA_BF), Manning's roughness coefficient for main channel flow (CH_N2) and Groundwater "revap" coefficient (GW_REVAP) were relatively less sensitive parameters in flow simulation. On the other hand, parameters such as Manning's "n" value for overland flow (OV_N), threshold water level in the shallow aquifer for return flow to occurs (GWQMN) and Effective hydraulic conductivity in the main channel (CH_K2) were found to be least sensitive in runoff yield simulation.

3.3.4. Model calibration for flow

Flow calibration was performed for a period of eight years from 01/01/1987 to 31/12/1994, within which the first two year were considered as a warm up period in order to set hydrologic processes to reach into equilibrium.

Observed daily stream flows were adjusted on the monthly basis using excel and Simulations runs were conducted on monthly basis to compare the modeling output with the measured monthly discharge at the outlet of Tikur Wuha watershed. Manipulation of the identified parameter values were carried out within the allowable ranges recommended by SWAT developers. The value of the selected sensitive parameters was changed so many times within the acceptable ranges until satisfactory results were met between the monthly simulation runs and monthly measured discharges.

After all these adjustments in SWAT model, the simulation was done and parameters were calibrated using SUFI2 in SWAT_CUP and the calibrated parameters were updated in the model and the final simulation was run using sensitive parameters.

The calibration results in Table 3 show that there is a good agreement between the simulated and measured monthly flows. Percent of error of the observed and simulated monthly flows at Tikur Wuha outlet was found as -16% which is well within the acceptable range of ±20%. Further a good agreement between observed and simulated monthly flows are shown by the coefficient of determinations (R^2=0.77) and the Nash-Suttcliffe simulation efficiency (ENS=0.70) and thus fulfilled the requirements suggested by Santhi *et al.* (2001) for R^2 >0.6 and ENS> 0.5.

Table 3: Calibration Statics for simulated flow on Tikur Wuha gauge station

Period	Mean monthly flow (m^3/s)		% Error	R^2	ENS
	Observed	Simulated			
1994-1999	6.6	5.5	-16	0.77	0.7

The graphical representation of the simulated and observed monthly flow was shown in Figure 13 indicating a reasonable agreement. Even though the model slightly overestimates the peak values in the months in August and September of 1987 and in the year 1992 (Figure 12), and underestimates in remaining part of the calibration period. The overall flow was well simulated and the trend shows good patterns.

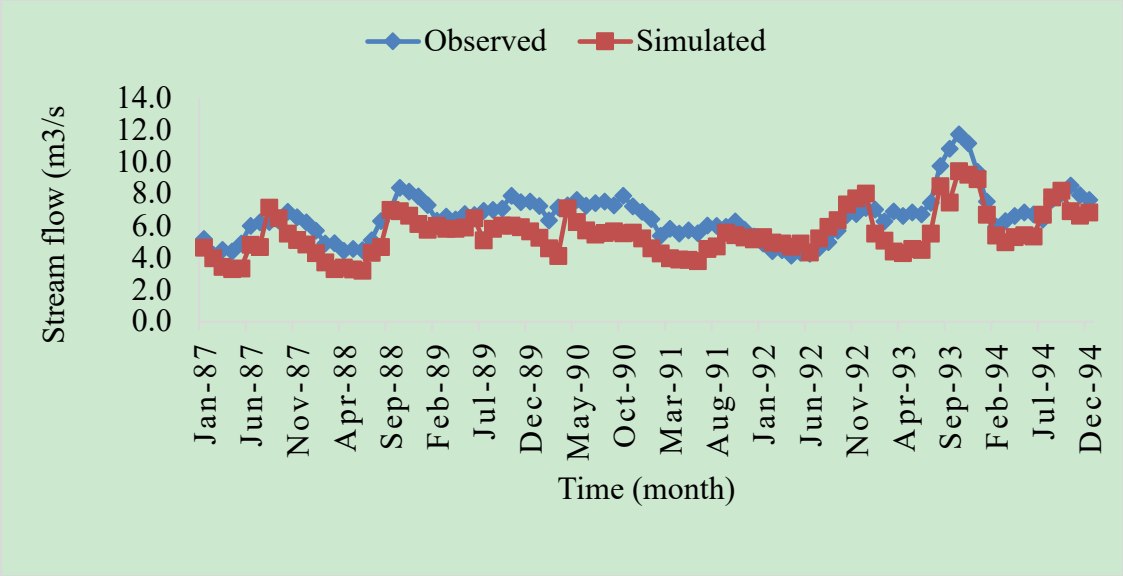

Figure 12: Calibration results of average monthly simulated and observed flows (1987-1994)

3.3.5. Model validation for flow

Validation of the model was carried out using an independent data set for five years from 1995-1999 without making further adjustments of sensitive parameters.

As it can be seen from Table 4, there is good agreement between monthly observed and simulated flows at Tikur Wuha River gauge station. The percent of error between the observed and simulated monthly flow was only -9% and it is found within the tolerable range of ±20%. The coefficient of determinations (R^2) and Nash-Sutcliffe simulation efficiency (ENS) were found to be 0.87 and 0.77 respectively and these shows a very good correlation of the simulation results with the observed values.

Table 4: Validation statics for simulated flow on Tikur Wuha gauge station

Period	Mean monthly flow (m^3/s)		% Error	R^2	ENS
	Observed	Simulated			
1994-1999	9.6	8.8	-9%	0.87	0.77

Even though the model slightly overestimates the peak values in 1995 and the month of August-November of 1998 and underestimates the remaining years, there was a good agreement between observed and simulated results (Figure 13).

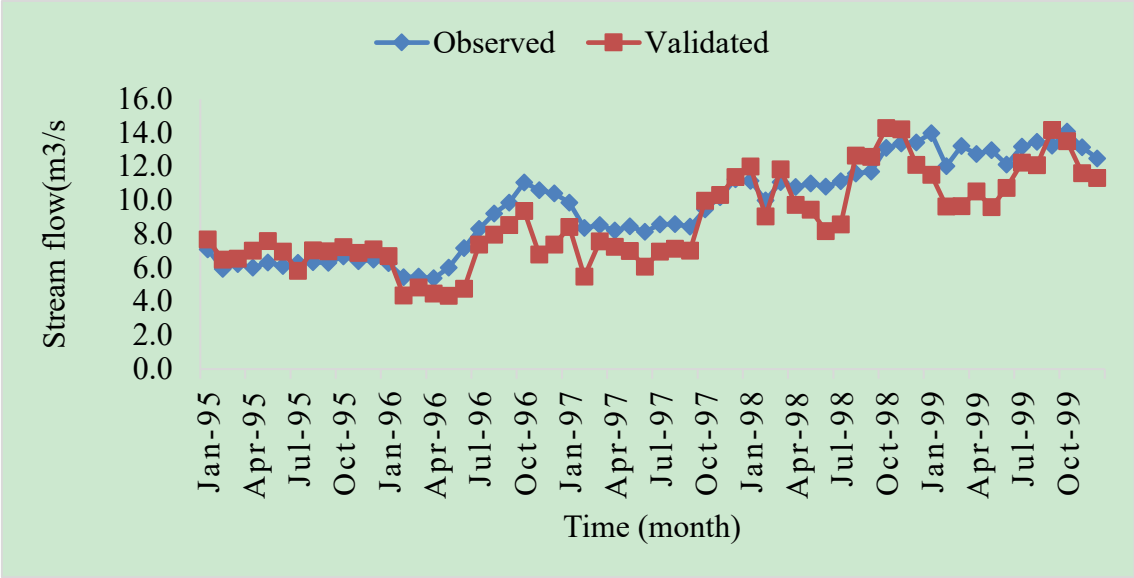

Figure 13: Validation results of average monthly simulated and observed flows (1995-1999)

Thus, the validation check illustrates the accuracy of the model for simulating time periods outside of the calibration period. The model performed as good in the validation period (1995-1999), as well as for the calibration period (1987-1994) at Tikur Wuha gauge station. Hence, the set of optimized parameters used during calibration process can be taken as the representative set of parameters to explain the hydrologic characteristic of the Tikur Wuha watershed and further simulations using SWAT model could be carried out by using these parameters for any period of time. Thus, the total annual stream flow and mean monthly stream flow of Tikur Wuha watershed were expected that 92.7m^3/s and 7.7 m^3/s in the base period respectively.

Based on SWAT model output, spatially the highest rate of discharge was occurred at Northern, Southern, Northwestern, and some central parts of the watershed. whereas the lowest discharge rate was occurred at central (plane areas), Parts of Northern and Southern of the watershed (figure 14). Vertic Luvisol was the major dominate soil existing in the area where the highest discharge was occurred. The dominant land use type and slope class where highest discharge occurred where agricultural land and 15-30% slope class respectively.

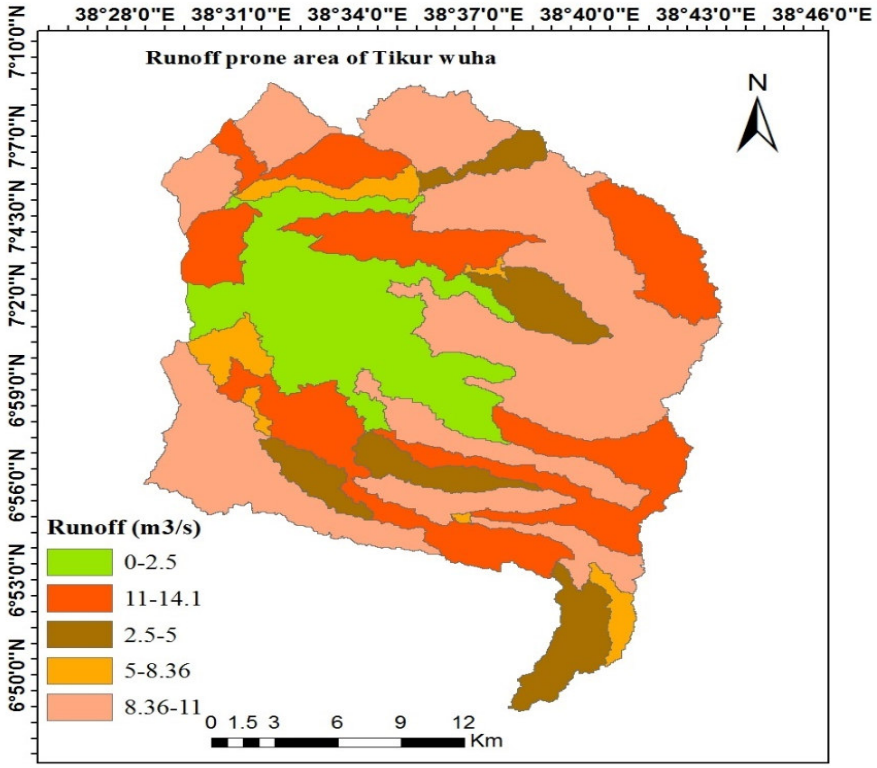

Figure 14: Spatial distribution of runoff in Tikur Wuha watershed

3.3.6. Impact of climate change on stream flow

The period from 1987–1999 were used as a base period against which the climate change impact was assessed. The daily precipitation and minimum and maximum temperature used for impact assessment were SDSM model results for the future three data periods of 34, 34 and 33 time series years (2000-2033, 2034-2067 and 2068-2100) respectively and SWAT hydrologic model was re-run for each data periods and the SWAT parameters identified during the calibration period also remains valued.

Other climate variables such as wind speed, solar radiation, and relative humidity were assumed constant throughout the future simulation periods, which are not possible in actual case (Abbaspour *et al*., 2007). Even though it is definite that in the future land use changes will also take place, this was also assumed constant.

For this study the impact of climate change on stream flow was predicted based on temperature and rainfall changes on monthly, seasonal, and annual basis. The simulation results for the future three time horizons in terms of monthly and annual average total flow volume are summarized in the Tables 5, 6 and 7 below.

Table 5: Mean monthly predicted Stream flow for RCP2.6 scenario

Year	Months												
	Jan	Feb	Mar	Apr	May	Jun	Jul	Aug	Sep	Oct	Nov	Dec	Total
Observed	7.7	6.6	7.0	6.8	7.1	7.1	7.5	8.0	8.3	9.1	8.8	8.6	92.7
2020s	8.1	5.6	7.9	6	8	7.2	13.1	8.9	8.9	9.6	9.4	7.9	100.5
2050s	8.4	5.4	7.9	5.4	8	7.9	12.4	12.8	9.2	9.9	9.6	8.1	104.9
2080s	8.8	5	8.1	8.1	8.8	6.1	13	11.2	10.3	10.3	9.6	7.4	106.8

Table 6. Mean monthly predicted Stream flow for RCP4.5 scenario

Year	Months												
	Jan	Feb	Mar	Apr	May	Jun	Jul	Aug	Sep	Oct	Nov	Dec	Total
Observed	7.7	6.6	7.0	6.8	7.1	7.1	7.5	8.0	8.3	9.1	8.8	8.6	92.7
2020s	10	6.2	7.9	6.9	9.8	6.9	12.3	10.5	9.9	9.6	10.1	8.6	108.7
2050s	11.1	6.9	7.7	6.4	10.3	6.7	12.6	12.8	10.5	10.2	10.8	9.2	115.2
2080s	10.7	5.1	11.2	6.1	10.6	7.1	12.3	13.5	10.5	11.8	11.5	10.9	121.4

Table 7. Mean monthly predicted Stream flow for RCP8.5 scenario

	Months												
Year	Jan	Feb	Mar	Apr	May	Jun	Jul	Aug	Sep	Oct	Nov	Dec	Total
Observed	7.7	6.6	7.0	6.8	7.1	7.1	7.5	8.0	8.3	9.1	8.8	8.6	92.7
2020s	7.9	6.7	8.8	7.4	6.3	9.8	12.9	8.7	9.9	8.8	11.3	7.9	106.4
2050s	7.4	6.4	9.5	9.2	6.6	11.3	12.2	11.9	12.2	10	10.1	8.8	115.7
2080s	8.6	5.6	10.2	10.1	6.7	11.6	13.8	15.4	11.1	12.8	10.8	9	126

As it can be seen from figure 15 (a, b and c) the results (2000-2100) for average annual total flow volume showed an increasing trend for RCP2.6, RCP4.5 and RCP8.5 scenarios as compared to the base period. The percentage increment of total average annual flow volume ranges from 8% (2000-2033) to 15% (2068-2100) for RCP 2.6 scenario, and for RCP4.5 scenario the increment ranges between 17% (2000-2033) and 31% (2068-2100). For RCP8.5 scenario the percentage of total annual increment of discharge volume ranging from 14% (2000-2033) and 35% (2068-2100). As compared to the base period, the mean annual flow volume results of this study confirmed the previous researches done by Beyene *et al. (*2010) and Dile *et al*. (2013) also showed that annual inflow volume on Gilgel Abay River increases in the future periods. In addition, this study in agreement with Kebede *et al.* (2014) in which the annual discharge on Tikur wuha river to the Lake Hawassa shows increasing trend.

On monthly basis, in the month of July to November the average monthly total flow volume increases throughout the future three time horizon for both RCP2.6, RCP4.5 and RCP8.5 scenarios as compared to the base period. The highest flow volume increment was recorded on the month of July up to 78% (2000-2033), 71% (2034-2067) and 88% (2068-2100) for RCP2.6, RCP4.5 and RCP8.5 scenarios, respectively. On the other hand, the decrement of flow was recorded for RCP2.6, RCP4.5 and RCP8.5 scenarios were recorded; For RCP2.6 scenario the slight decrement showed on the months of December up to 8 %, 5% and 13% for 2020s, 2050s and 2080s respectively. For RCP4.5 scenario the highest decrement recorded on the month of February up to 15%, 5% and 29% for 2020s, 2050s and 2080s respectively. For RCP8.5 the decrement reaches up to 8%, 12% and 22% respectively, in the month of February.

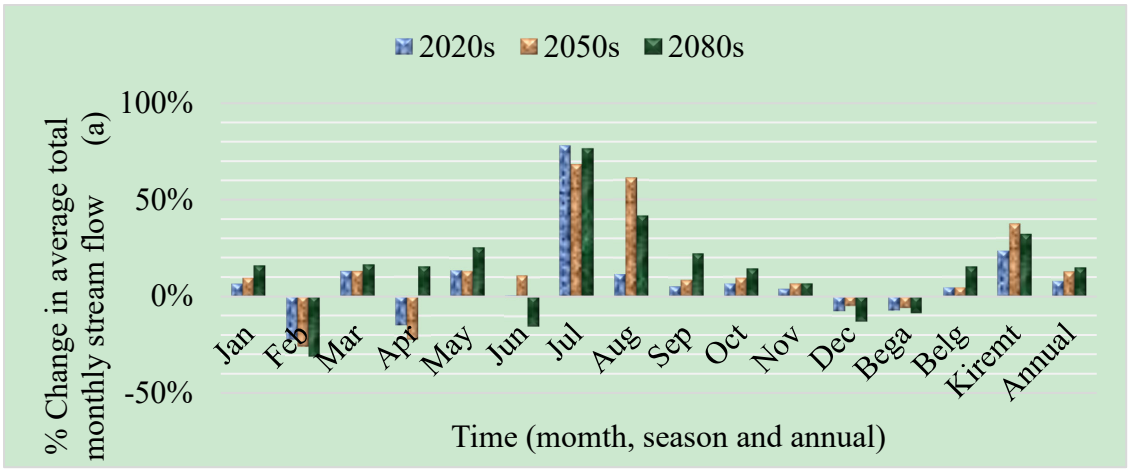

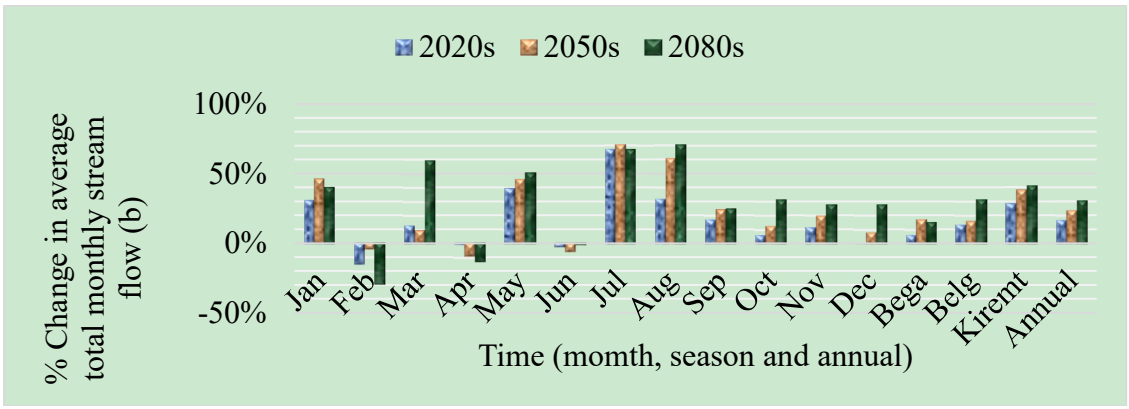

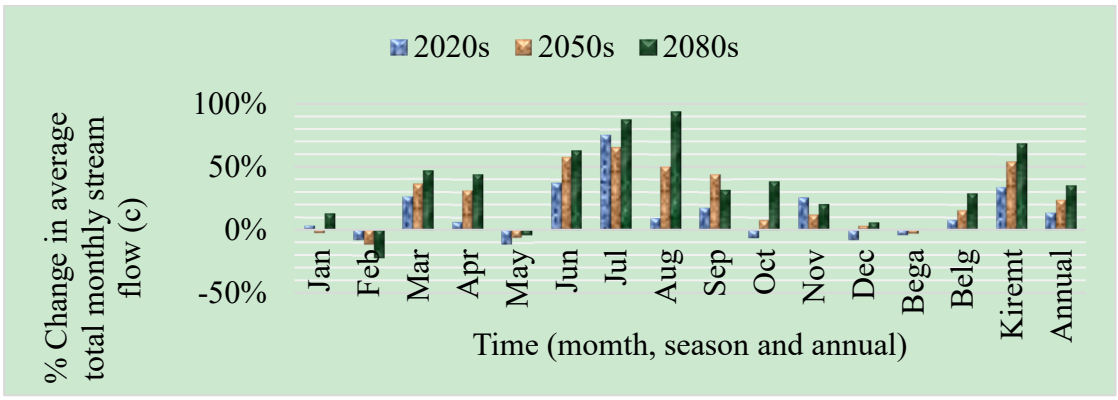

Figure 15: Change in average stream flow for the period 2000-2100 as compared to the baseline period (1987-1999) at Tikur Wuha watershed for RCP2.6 (a), RCP4.5 (b) and RCP8.5 (c) scenario.

Seasonally, the average total flow volume increases in Belge and Kermit season. In Bega season (the slight decrement for RCP2.6 and RCP8.5 scenarios) for future time horizons. However, the highest increment is shown in Kermit season (June-September) in which the percentage change ranges between 32-37% (2068-2100), 38-41% (2068-2100) and 54-68% for RCP2.6, RCP4.5 and RCP8.5 scenario respectively. The percent of increment for RCP8.5 (high emission) scenario was higher than RCP2.6 (medium to low) and RCP4.5 (medium emission) scenarios. This study reveals the increment of flow volume during Belg season in line with (Tekle, 2014).

Rizwan *et al*. (2010) carried out research in northern part of Ethiopia on the upper Blue Nile using different GCM out puts including HadCM3 and canESM2 and the results showed that the runoff increases in the future in the major rainy seasons (June-September) which causes the possibility of flood occurrences in the future due to extreme runoff. This study also reveals the increment of runoff in Kiremt season in line with (Rizwan et al., 2010).

In general, climate change results in an increase in flow volumes on Tikur wuha River. Meanwhile, the increase in flow will feed significant amount of inflows for the Lake Hawassa. However, the increase inflow volume of Tikur Wuha River is more significant in “Belg and Kiremt” which may cause flooding problems on Hawassa town and surrounding agricultural land. Therefore, with climate change the runoff of Tikur Wuha River

may become much more seasonal and as a result the flow of the River may highly reduce in some months and season while the flow highly increases in some part of the year.

3.3.7. Spatial distribution of simulated sediment yields in Tikur Wuha watershed

Even though calibrations and validation of sediment yield was not performed, the model runs were done for a period of 13 years (1987-1999). The Simulated output of sediment yields of each sub-watershed areas were identified in Tikur Wuha watershed. Identifying erosion prone areas in the watershed enables the watershed management to be applied to the proper areas to reduce the sediment yield. Spatial analysis of sediment prone areas is one of the many tasks SWAT can do while modeling sediment. SWAT is powerful in spatial visualization of sub basin or HRU level detail so that one can see which area produces high sediment and which area produces less.

The 13 years average simulated annual suspended sediment generated were 15.79 tons/ha/yr. From 69 sub-catchments of Tikur Wuha watershed, one sub-watershed generated an average annual sediment yield of 28.31 t/ha/yr (sub basin 3) while, 34 sub-watersheds generated average annual sediment yield ranging from 0.42-9.11 ton/ha/yr, 23 sub watersheds generated average annual sediment yield ranging from 11.23-19.22 and the remaining 11 sub-watersheds generate average annual sediment yield ranging from 22.22-26.27 t/ha/yr.

According to FAO (2006), degree of erosion classification the class assigned to the annual sediment yield map of the study area was reclassified in to five major categories of soil erosion hazard areas such as none to slight (0.4-9 t/ha/yr), slight (10-20 t/ha/yr), moderate (21-50 t/ha/yr), severe (50-75 t/ha/yr) and very severe (more than 75 t/ha/yr). Based on this classification, the degree of erosion in Tikur Wuha watershed was classified as, none to slight (49.27%), slight (33.33%) and moderate (17.4 %). Therefore, similar study in Ethiopia indicate that soil erosion by water represents a major threat to the long-term productivity of agricultural and water bodies in the Ethiopian highlands where the estimated soil erosion rates ranges from 16 t ha^{-1} y^{-1} to as much as 300 t $ha^{-1}y^{-1}$ (Hurni, 1993).

In addition, the ranges of tolerable soil loss level for various agro-ecological zones of Ethiopia were found from 2-18 t/ha/yr (Hurni, 1993). In average, Tikur wuha watershed generated an average annual sediment yield up to 15.79 ton/ha/year, it is under tolerable range. But, the simulated soil loss rate of some of sub-watersheds of Tikur Wuha watershed exceeds the maximum tolerable soil losses rate of 18 tons/ha/yr. This indicates that soil erosion is a serious problem of the study area. Thus, among all sub-watersheds that indicated in Tikur Wuha watershed Northern, Northeastern, Southern and Southwestern parts of the watershed are at risk to soil erosion (see Figure 16).

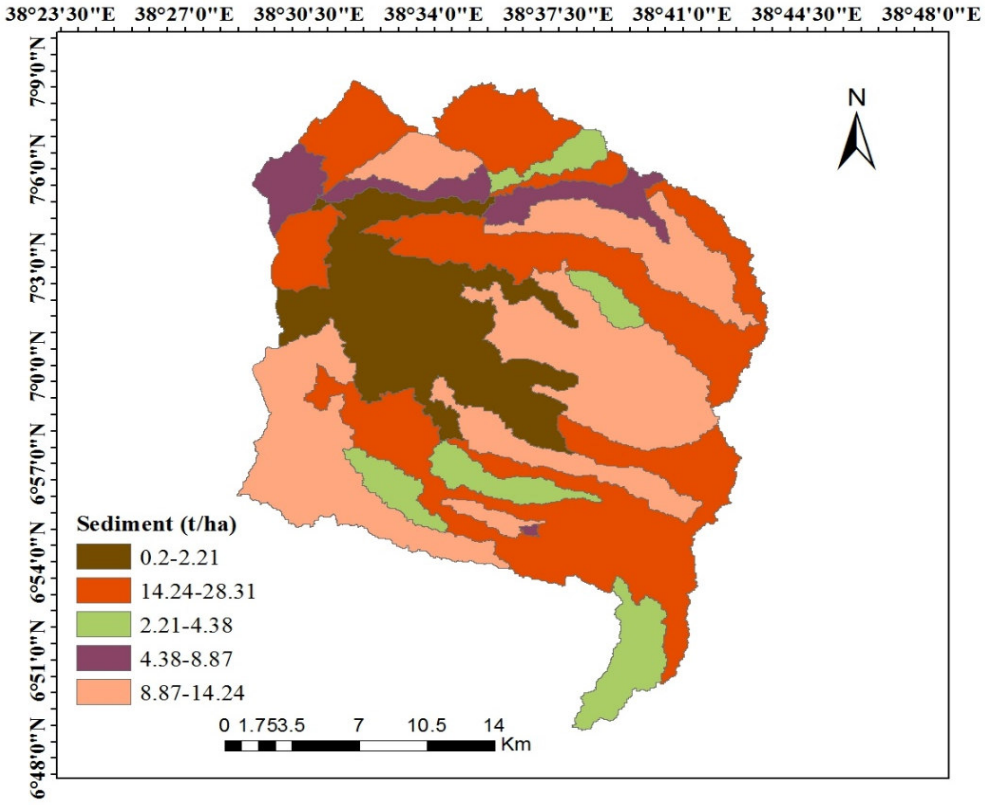

Figure 16: Spatial distribution of simulated sediment yields in sub basins (1987-1999)

Daily weather data, soil and land use/land cover data were used in the SWAT model. The model had been run both annually and monthly for the mentioned period and several types of output had been produced. Figure 18 represents the predicted value of average annual sediment yield. It can be concluded that the same trend had been assessed for inflow and sediment yield simulation; this indicate that the two processes are strongly related. The maximum flow and sediment yield correspond to in sub basin 3 which is more of agricultural land and its slop range 15-30%. The simulated future sediment yield indicated on figure 17 (a, b, c) for RCP2.6, RCP4.5 and RCP8.5 scenarios.

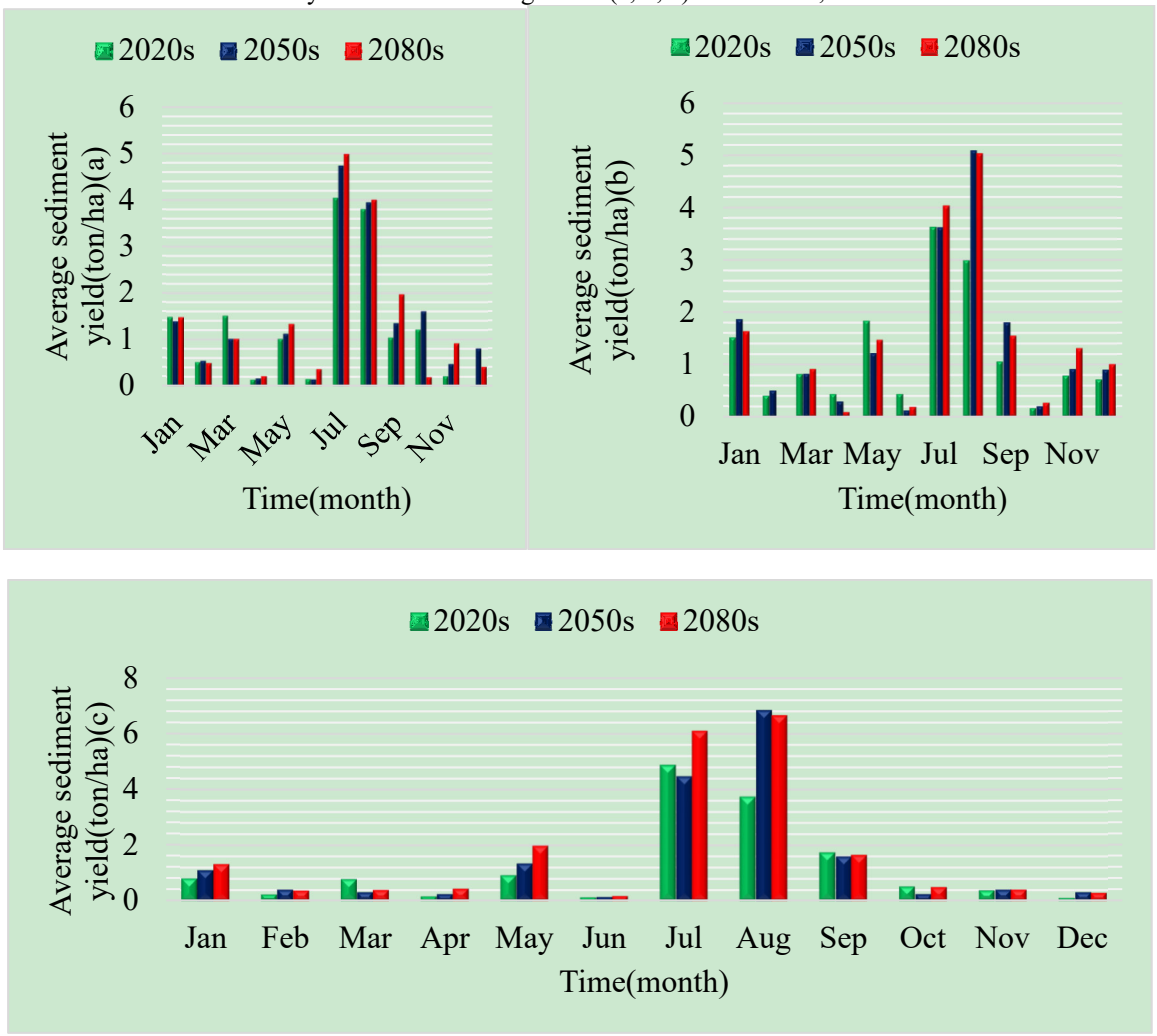

Figure 18: Simulated mean annual sediment yield for RCP2.6 (a), RCP4.5 (b) and RCP8.5 (c)

In future period, the predicted average annual sediment yield from the watershed would have been 16.80 tons/ha/yr. Depending on this the average annual sediment yield; a total amount of 1.05×10^8 tons would have been transported to the outlet of the watershed or inlet of Lake Hawassa during the period 2000 to 2100 (with in one hundred one years).

4. CONCLUSIONS AND RECOMMENDATIONS

4.1. CONCLUSION

The result of this study showed a general increasing trend for precipitation, maximum and minimum temperatures in all three time periods (2020s, 2050s and 2080s). The precipitation showed that increasing trends for the future time horizons mainly in the major parts of the rainy season (June to September), Seasonally in Belg and Kiremt season while it decreases in Bega season. The increment of precipitation in these seasons may be a good opportunity for agriculture; however, increment of temperature, flow volume and sediment yield may affect the area.

Due to climate change, the average monthly, seasonal and annual inflow volume changes mainly increase within the increasing of precipitation. Tikur Wuha watershed generates an average flow of 7.7 m^3/s and the average annual sediment yield of 15.79 tons/ha for the base periods. In the future period, the predicted average annual sediment yield from the watershed will be 16.80 tons/ha/yr transported to Lake Hawassa from the period 2000 to 2100. It is the higher sediment yield which affect the Lake; by rising the sea-level and flooding around agricultural

areas mainly during rainy season (June- September). In addition, the simulated soil loss rate of some of sub-watersheds of Tikur Wuha watershed exceeds the maximum tolerable soil losses rate. This indicates that soil erosion is a serious problem of the study area. Thus, among all sub-watersheds that Northern, Northeastern, Southern and Southwestern parts of the watershed are at risk to soil erosion for the future periods. In general, this study confirmed that climate change is likely to have severe impact on the hydrologic flow of Tikur wuha watershed.

4.2. RECOMENDATIONS

Knowing the seasonal simulated long term average annual precipitation, temperature, stream flow and sediment yield components in the future is useful to recommend better alternative and complementary action of climate change. Keeping in view, the threats to the survival of Tikur Wuha watershed and Lake Hawassa, the following points are recommended for its proper conservation and management.

- Afforestation around the Cheleleka wetland and adoption of soil conservation measures around erosion prone areas of the watershed to prevent siltation of the Lake Hawassa. This will help to maintain ecological balance besides preventing sediment deposition. It will also improve the productivity of the ecosystem.
- Future work need to consider also studying the effects of different climate change adaptation strategies.
- The models and model outputs used in this study possessed a certain level of uncertainty. The model simulation considered land use changes and other climatic variables such as wind speed, sunshine hours, and relative humidity remain constant for the future time horizons although it is not true in the actual case. Hence, the results of this research should be taken carefully and be considered as indicative prediction of the future and further researches should be extended by considering the future land use changes and other climatic variables. In addition, lack of recorded sediment data, calibration and validation of sediment yield not possible.
- The results of this study are based on the outputs of a single GCM. However, it is recommended to use different GCM outputs to compare the results of different models that would result different hydrological impacts. Meanwhile, the GCM was downscaled to a catchment level only using statistical downscaling model which is a regression based model, even though other methods exists which are used for impact assessment. Thus, this research should be extended in the future considering other downscaling methods.
- As mentioned above, lack of sediment data was the major challenges of this study. Hence, any of the concerned bodies should give due attention to data recording and even for data handling (reliable data).

5. REFERENCE

Abbaspour, K.C. 2007. User manual for SWAT-CUP, SWAT calibration and uncertainty analysis programs. *Swiss Federal Institute of Aquatic Science and Technology, Eawag, Duebendorf, Switzerland*.

Ashenafi, A. A. 2014. *Modeling hydrological responses to changes in land cover and climate in Geba river Basin, Northern Ethiopia* (Doctoral dissertation, Freie Universität Berlin).

Benestad, R.E., Hanssen-Bauer, I. and Chen, D. 2008. *Empirical-statistical downscaling*. World Scientific Publishing Company.

Beyene T, Lettenmaier D. and Kabat P. 2010. Hydrological impacts of climate change on the Nile River Basin: Implications of the 2007 IPCC scenarios. Clim Chang 100: 433–461.

Dile, Y.T., Berndtsson, R. and Setegn, S.G., 2013. Hydrological response to climate change for gilgel abay river, in the lake tana basin-upper Blue Nile basin of Ethiopia. *PloS one*, *8*(10): e79296.

Dingman, S.L. 2002. Physical hydrology, second edition. Unpublished book.

Dixon, B. and Earls, J. 2012. Effects of urbanization on streamflow using SWAT with real and simulated meteorological data. *Applied Geography*, *35*(1-2): 174-190.

Enyew, B.D., Van Lanen, H.A.J. and Van Loon, A.F. 2014. Assessment of the impact of climate change on hydrological drought in Lake Tana catchment, Blue Nile basin, Ethiopia. *J. Geol. Geosci 3*: 174.

FAO (Food and Agriculture Organization). 2006. World reference base for soil resources. World Soil Resources Report 103. Rome: Food and Agriculture Organization of the United Nations: 132.

Gumindoga, W., Rwasoka, D.T., Nhapi, I. and Dube, T. 2017. Ungauged runoff simulation in Upper Manyame Catchment, Zimbabwe: Application of the HEC-HMS model. *Physics and Chemistry of the Earth, Parts A/B/C*, *100*: 371-382.

Hurni, H. 1993. World Soil Erosion and Conservation: Land degradation, famine, and land resource scenarios in Ethiopia.

Intergovernmental Panel on Climate Change. 2014. *Climate Change 2014–Impacts, Adaptation and Vulnerability: Regional Aspects*. Cambridge University Press.

IPCC, 2007. The Fourth Assessment Report of the Intergovernmental Panel on Climate Change. *Geneva, Switzerland*.

IPCC, 2007. The physical science basis: summary for policymakers. Geneva: Intergovernmental Panel on Climate Change secretariat.

IPCC-TGICA. 2007: General Guidelines on Use of Scenario Data for Climate Impact and Adaptation Assessment.Version 2. Prepared by T.R.Carter on behalf of the IPCC on Climate Change, Task Group on Data and Scenario Support for Impact and Climate Assessment: 66.

Kebede, W., Tefera, M., Habitamu, T. and Alemayehu, T. 2014. Impact of land cover change on water quality and stream flow in Lake Hawassa watershed of Ethiopia. *Agricultural Sciences*, *5*(08): 647.

Kim, U., Kaluarachchi, J. J.and Smakhtin, V. U. 2008. Climate change impacts on hydrology and water resources of the Upper Blue Nile River Basin, Ethiopia. Colombo, Sri Lanka: International Water Management Institute (IWMI Research Report 126):27.

Liu, J., Chen, S., Li, L. and Li, J. 2017. Statistical Downscaling and Projection of Future Air Temperature Changes in Yunnan Province, China. *Advances in Meteorology*, *2017*.

Meinshausen, M., Smith, S.J., Calvin, K., Daniel, J.S., Kainuma, M.L.T., Lamarque, J.F., Matsumoto, K., Montzka, S.A., Raper, S.C.B., Riahi, K. and Thomson, A.G.J.M.V. 2011. The RCP greenhouse gas concentrations and their extensions from 1765 to 2300. *Climatic change*, *109*(1-2): 213.

Mekonnen, D.F. and Disse, M. 2016. Analyzing the future climate change of Upper Blue Nile River Basin (UBNRB) using statistical down scaling techniques. *Hydrology and Earth System Sciences Discuss*.

Nawaz, N.R., Bellerby, T., Sayed, M. and Elshamy, M. 2010. Blue Nile runoff sensitivity to climate change. *Open Hydrology*, *4*: 137-151.

Riahi, K., Grübler, A. and Nakicenovic, N. 2007. Scenarios of long-term socio-economic and environmental development under climate stabilization. *Technological Forecasting and Social Change*, *74*(7): 887-935.

Rizwan, N., Timothy, B., Mohamed Sayed and Mohamed Elshamy. 2010. Blue Nile Runoff Sensitivity to Climate Change. *Open Hydrology Journal*, 2010, 4: 137-151.

Santhi, C., Arnold, J.G., Williams, J.R., Dugas, W.A., Srinivasan, R. and Hauck, L.M. 2001. validation of the swat model on a large RWER basin with point and nonpoint sources 1. *JAWRA Journal of the American Water Resources Association*, *37*(5): 1169-1188.

Taye, M. T. 2010. Hydrological modeling of climate change impact on selected catchment of Nile River basin. Journal of Hydrology and Earth System Sciences Discussions 7, 5441–5465. doi:10.5194/hessd-7-5441-2010.

Tekle, A. 2014. Assessment of climate change impact on water availability of Bilate watershed, Ethiopian Rift Valley Basin. In *AFRICON, 2015*: 1-5.

Wayne, G. P. 2013. The beginner's guide to representative concentration pathways. *Skeptical science*, 25p.

Wilby, R.L. and Dawson, C.W. 2007. SDSM 4.2-A decision support tool for the assessment of regional climate change impacts. *User Manual. London, UK*.

Wilby, R.L., Dawson, C.W. 2004. Using SDSM - A decision support tool for the assessment of regional climate change impacts.